RADIOTRONICS

Vol. 29, No. 1 January, 1964

IN THIS ISSUE

AN AWV PUBLICATION

1

REGISTERED IN AUSTRALIA FOR TRANSMISSION BY POST AS A PERIODICAL.

Theory and Application of Electron Tunneling

by R. E. COLLINS, B.Sc. (Hons.)
AWV Physical Laboratory

A qualitative discussion of the electron tunneling effect in solids is given. The method of calculating tunneling probability in various particular cases is outlined.

The properties of several different kinds of tunnel devices are discussed. The simplest type of device, the tunnel cathode, consists of two metal layers separated by a thin insulating film. A potential difference between the two metals causes electrons to tunnel from the one at lower potential to the one at higher potential. Electrons, having tunneled into the second metal film, can traverse this film if it is thin enough, and be emitted into vacuum. The energy distribution of the emitted electrons has been measured and, from these results, it is possible to obtain values for the mean free path between collisions for hot electrons in a metal as a function of electron energy. These values can be correlated with those obtained by measurements of photo excited electrons.

Two other tunnel devices having possible future application are described. These are a three terminal transistor-like device, consisting of successive layers of metal-insulator-metal-semiconductor and a device consisting of layers of semiconductor-metal-semiconductor. Although the work on these devices is still in the preliminary stages, they both show promise of having useful application in electronic circuitry.

Introduction

The phenomenon of electron tunneling has received considerable attention in recent years, and several different kinds of device which depend for their operation on this effect have been proposed and constructed. Some of these devices have potential application in electronic circuitry; all of them furnish us with more information on the fundamental processes which take place during electron transfer in metals, insulators and semiconductors.

It is the purpose of this paper to discuss the mechanism of electron tunneling and to investigate the operation and potential application of several different kinds of tunnel device.

Electron Tunneling

In a solid, consideration of the interaction of electrons with the field due to the lattice shows that the possible electronic energies fall into a series of allowed bands separated by bands of forbidden energy. For net electron transport to take place there must be available energy levels immediately above the highest filled level, into which electrons can be excited by an applied electric field.

For normal conduction to take place between two parts in a solid, available energy levels must exist everywhere between these parts. However, even though there may be a region between the two parts in which there are no allowed energy levels, electron transport is still possible through this region if it is thin enough. This transport takes place by the quantum mechanical process of electron tunneling.

Uncertainty principle

In classical mechanics, it is assumed that all physical properties of a particle can be exactly specified at any given instant. For example, there is assumed to be no limit to the accuracy to which the position and momentum of a particle can be simultaneously specified. However, a fundamental principle of quantum mechanics states[1] that if the

1. See for example, Mott, N. F. and Sneddon, I. N., "Wave Mechanics and its Applications", Oxford, 1948.

position, x, of a particle is specified exactly, it is not possible to say anything about the particle's momentum, p_x. More generally, if there is an uncertainty, Δx, in the measurement of a particle's position, there must be a corresponding uncertainty Δp_x in its momentum, and these two quantities are related by the equation

$$\Delta x \times \Delta p_x > h/2\pi \qquad (1)$$

where h is Planck's constant (6.63×10^{-27} erg sec.).

From the Uncertainty Principle, a particle cannot be thought of as being completely localized in space, but is considered to be "smeared out" over a finite distance with a certain probability of finding the particle at any point. Quantum mechanics furnishes a method of calculating this probability.

In order to calculate the probability of finding an electron at a given point, it is necessary to represent the electron as a wave, $\psi(x, y, z, t)$. (In the following we assume that ψ is independent of time and treat only the one dimensional case of steady state motion in the x-direction; hence $\psi = \psi(x)$.) ψ must satisfy Schrödinger's wave equation,

$$\frac{d^2\psi(x)}{dx^2} + \frac{2m}{\hbar^2}[W - V(x)]\psi(x) = 0, \left(\hbar = \frac{h}{2\pi}\right) \qquad (2)$$

where W is the energy of the electron and V(x) is the potential energy of the electron in the external field. The solution of this equation is subject to the boundary condition imposed by the particular problem.

The results of quantal calculations are interpreted on the basis that the probability of finding a particle in unit volume is proportional to $|\psi|^2$.

Tunneling probability

Consider an electron of energy W incident on a rectangular potential barrier of height V_o, extending from $x = 0$ to $x = a$, Fig. 1 (a). According to classical mechanics, if $V_o < W$, the electron will pass over the barrier, and if $V_o > W$, the electron will be reflected at the barrier and will return along its initial path. However, in quantum mechanics, this is not the case, and there is a finite probability of finding the electron in the region $x > 0$, even though the energy of the electron is less than the barrier height. The wave function of the electron decays exponentially for $a \geqslant x \geqslant 0$, but if the barrier is thin enough, it will still be finite at $x = a$ and there will be a finite probability of the electron having tunneled through the barrier and being detected in the region $x > a$.

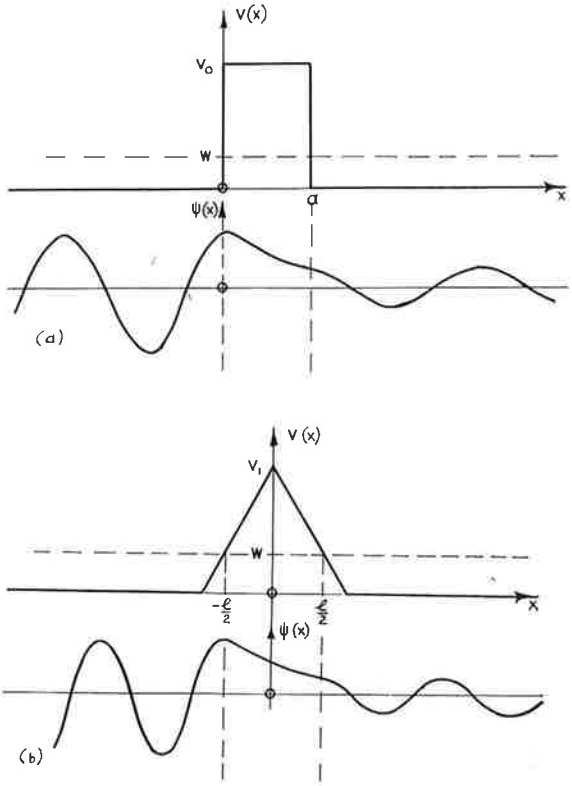

Fig. 1 — Potential barrier and electron wave function; (a) rectangular barrier, (b) triangular barrier.

It is possible to calculate exactly the probability of tunneling in only a few special cases, e.g. a rectangular barrier. In practice, barriers seldom have such a simple shape, and approximate methods must be used. The most useful method is that due to Wentzel, Kramers and Brillouin (the WKB method) which gives the result that for a barrier V(x), Fig. 2, the tunneling probability of an electron of energy W is

$$P(W) = \exp\left\{-2(2m/\hbar^2)^{\frac{1}{2}}\int_{x_2}^{x_1}[V(x) - W]^{\frac{1}{2}}dx\right\} \qquad (3)$$

where x_1 and x_2 are the points where $V(x) = W$. This approximation is only valid when V—W changes by a small amount in a distance comparable with

$$h\{2m(V - W)\}^{-\frac{1}{2}}.$$

The tunneling probability through a barrier is the same in either direction for electrons of the same energy. Thus, total tunnel current density through a barrier is

$$j = e\int_0^\infty \{N_1(W) - N_2(W)\}P(W)dW \qquad (4)$$

where $N_1(W)dW$, $N_2(W)dW$ are the number of electrons of energy between W, W + dW impinging on the barrier on the two sides, per unit area per unit time, and e is the charge on one electron.

It should be noted that an implicit assumption in this argument is that there are vacant energy states beyond the barrier that tunneled electrons can occupy. If there are no states present at the energies under consideration, or if the states present are already filled by electrons, tunneling cannot take place.

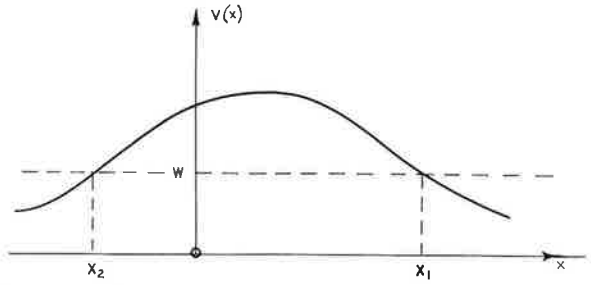

Fig. 2 — Slowly-varying potential barrier—the WKB approximation.

Applications of Electron Tunneling

The tunnel cathode

A simple device depending for its operation on electron tunneling is the tunnel cathode, which consists of alternate layers of metal-insulator-metal deposited on an insulating substrate, Fig. 3 (a). In a typical device, the lower metal, M1, is a thick film of aluminium, the insulating layer, I, is anodically formed aluminium oxide ~ 100 A° thick, and the upper film, M2, may be any of a number of metals, e.g. aluminium or gold.

The band structure of such a device under zero bias is shown in Fig. 3 (b). ϕ is the metal-insulator work function, and ϕ^* is the metal-vacuum work function. When a potential difference V, of the order of several volts is applied between the two metal films, so that the upper metal is made positive with respect to the lower metal, the potential barrier for electrons with energies near the Fermi level in M1 may assume the triangular shape shown in Fig. 3 (c) to a first approximation. Electrons have a finite probability of tunneling through this narrowed potential barrier into the conduction band of the insulator, from where they move into the upper metal film, M2. These are "hot" electrons in M2, as they have energies several electron volts above the Fermi level. Electrons may be scattered in energy both in the insulator conduction band and in the upper metal. If M2 is sufficiently thin ($\lesssim$ 1000 A° for aluminium), some electrons will reach the opposite side with sufficient energy to surmount the work function barrier of the film (~ 4ev for aluminium) and these electrons are emitted into vacuum.

Several successful attempts to construct tunnel cathodes have been made[2–7]. In most of these experiments the total emitted current density was very small ($\lesssim 10^{-3}$ a/cm^{-2}) although experiments with very thin upper metal films have yielded larger values of emitted current density.

It is found that emitted current density increases exponentially with tunnel voltage over several orders of magnitude. Tunnel current is also observed to increase exponentially with tunnel voltage, and it is found that the ratio of emitted current to tunnel current, α, is approximately

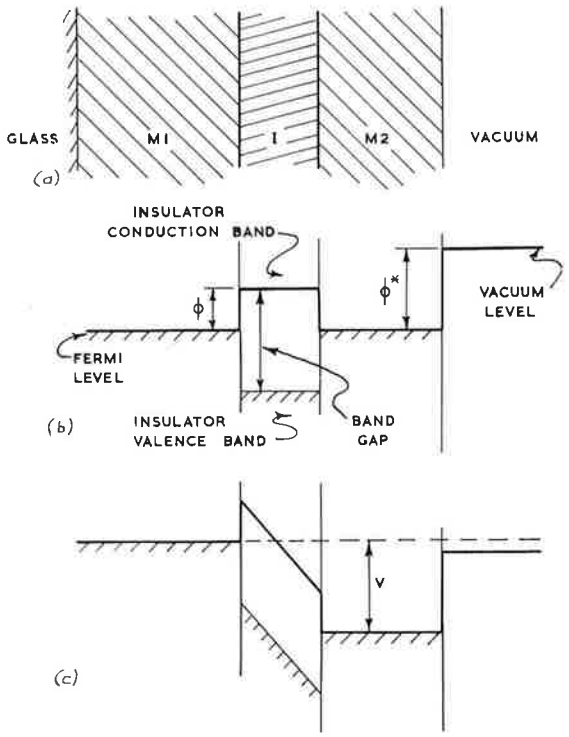

Fig. 3 — The tunnel cathode; (a) schematic cross section; (b) energy diagram, zero bias; (c) energy diagram with applied voltage V greater than metal-vacuum work function ϕ^*.

2. Mead, C. A., "The Tunnel Emission Amplifier", *Proc. I.R.E.*, 48, March, 1960, 359-361.
3. Mead, C. A., "Operation of Tunnel Emission Devices", *J. Appl. Phys.*, 32, April, 1961, 646-652.
4. Mead, C. A., "Transport of Hot Electrons in Thin Gold Films", *Phys. Rev. Letts.*, 8, Jan. 15, 1962, 56-57; *Phys. Rev. Letts.*, 9, July 1, 1962, 46.
5. Cohen, J., "Tunnel Emission into Vacuum", *J. Appl. Phys.*, 33, June, 1962, 1999-2000; "Tunnel Emission into Vacuum II", *Appl. Phys. Letts.*, 1, Nov. 1, 1962, 61-62.
6. Kanter, H. and Fiebelman, W. A., "Electron Emission from Thin Al-Al_2O_3-Au Structures", *J. Appl. Phys.*, 33, Dec., 1962, 3580-3588.
7. Hájek, Z. and Eckertová, L., "The Construction of a Stable Field Effect Cathode", *Naturwiss.*, 49, May, 1962, 201.

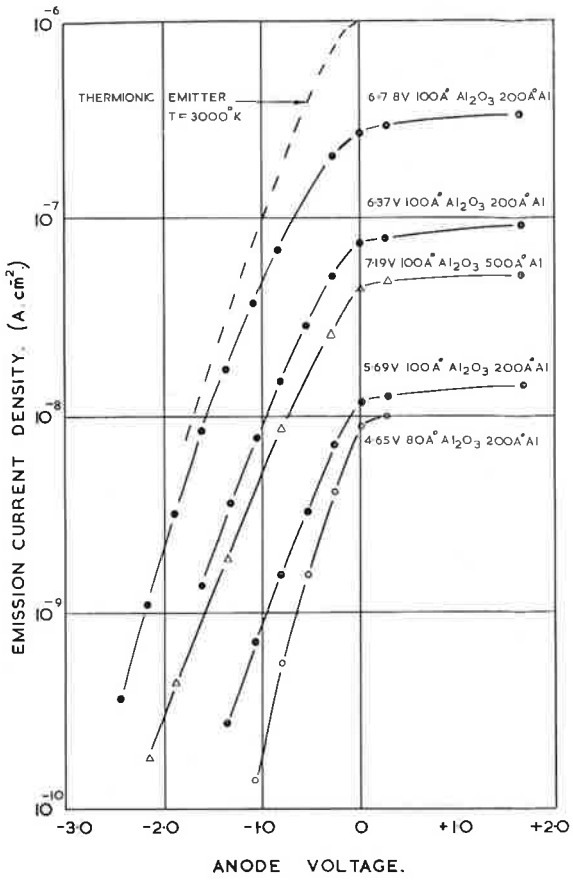

Fig. 4 — Retarding field characteristics for tunnel cathodes, comparison with thermionic emitter.

constant for a given upper film thickness of either gold or aluminium.

In measurements of electron emission, an anode is positioned in front of the emitter. When the anode is held several volts positive with respect to M2, all the emitted electrons are collected. If the anode potential is reduced to zero and then made negative, some of the emitted electrons have insufficient energy to reach the anode, and these return to the cathode. As the anode is made more negative, still more of the electrons return to the cathode and in this way it is possible to measure the energy distribution of the emitted electrons.

Typical results of such measurements made in this laboratory for aluminium-aluminium oxide-aluminium structures are shown in Fig. 4. The number of emitted electrons with energy greater than a given value is found to decrease approximately exponentially as the anode voltage is made more negative. The relative spread energy of the emitted electrons is found to depend on the oxide thickness, the upper film thickness, and the applied voltage.

The tunneled electrons entering the insulator conduction band are calculated to have an energy distribution of half width only a few tenths of an electron volt, centered near the Fermi level of the lower metal (Appendix 1), so that most of the large observed spread in the energy of the emitted electrons is due to scattering in the insulator conduction band and/or in the upper metal film. In principle, from these measurements it is possible to calculate the mean free path of hot electrons in a metal as a function of energy above the Fermi level.

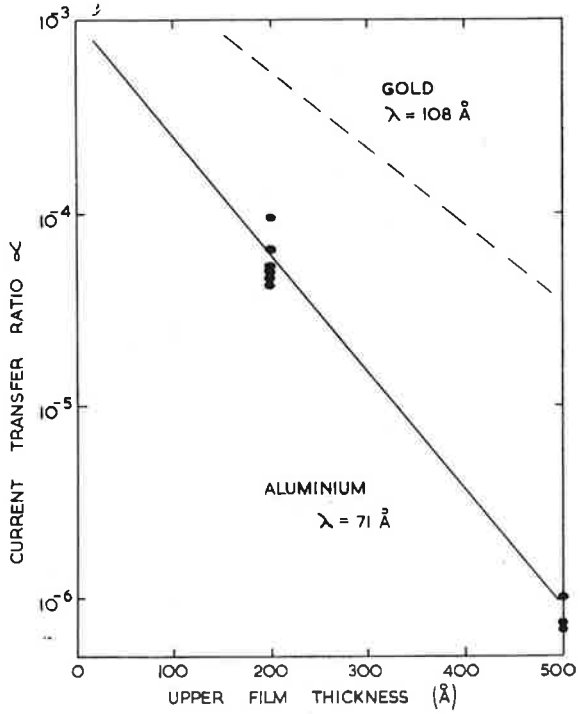

Fig. 5 — Variation of current transfer ratio with upper film thickness.

The ratio, α, of emitted current to tunnel current for different upper film thicknesses has been measured[4, 8] (Fig. 5). α decreases exponentially with thickness showing that the number of excited electrons decay exponentially with distance x_1 into M2, i.e.,

$$N(x_1) = N(x_0) \exp\{-(x_1 - x_0)/\lambda\} \qquad (5)$$

In this equation, λ is an attenuation length for hot electrons in the metal, averaged over energies $\geqslant \phi^*$. For aluminium[8], the mean free path is 75 A°, for gold[4] it is 106 A°, in both cases for electrons with energy between ~ 4ev and 6ev above the Fermi level.

Mean free paths of hot electrons in metals have also been measured by a photoexcitation method[9, 10], in which the hot electrons are excited photoelectrically in a thin gold film evaporated on a clean silicon surface. These measurements give a mean free path of 740 A° in gold, which

is much higher than that observed in tunneling experiments. However, tunnel emission experiments involve electrons at least 4ev above the Fermi level, while the photoexcited electrons have energies less than 1ev above the Fermi level. Theoretical considerations[11] show that scattering will be more pronounced for higher energy electrons which will thus exhibit a shorter mean free path, as observed.

Maximum observed dc current densities from tunnel cathodes with upper film 200 A° thick are ~ 1 ma/cm^{-2}, and most devices are destroyed below this level. Higher densities are obtainable with thinner upper films and Mead[4] reports emitted currents of ~ 1 a/cm^{-2}. All units are invariably destroyed at high tunnel current densities due to internal heating and so greater emission currents could be observed on a pulse basis. Using a combination of very thin upper films and pulse techniques, current densities of 100 a/cm^{-2} have been observed[7].

It is interesting to note that if the current transfer ratio α is extrapolated back to zero upper film thickness, values as small as 10^{-2} to 10^{-3} are obtained. This indicates that scattering in the insulator conduction band does in fact cause the tunneled electrons to suffer large energy losses, so that upon entering M2, only a small fraction still have energy greater than ϕ^*. If a suitable insulating film could be found, in which excited electrons were not so violently scattered, this limitation on the efficiency of the device would be removed.

Another reason for the low current densities observed is that only those electrons with energies greater than the work function of M2 are emitted into vacuum. For aluminium and gold, the work function is > 4ev. If the work function could be substantially lowered, a large increase in emitted current would be observed, and in fact, experiments in which caesium (work function ~ 2ev) has been placed on the surface of M2 have led to an increase in emitted current densities of from 3 to 5 orders of magnitude[5, 6, 8].

While it appears that further developments may produce a device capable of emitting high current densities, the large spread in the energies of the emitted electrons may render the tunnel cathode unsuitable as a low noise source of electrons. The magnitude of the energy spread of the emitted electrons can be seen from the slope of the dashed line in Fig. 4, which represents the retarding field characteristics which would be observed if the cathode was a thermionic emitter at 3000° K.

The metal-interface amplifier

A three-terminal active tunnel device which gives gain > 1 consists of alternate layers of metal-insulator-metal-semiconductor[12–14]. A typical device consists of an etched germanium substrate onto which is evaporated a very thin (100 A°) film of aluminium. This film is allowed to oxidise thermally to form an insulating layer some 20 A° thick, and a gold film is evaporated onto the oxide to form a source of electrons. The band structure of such a device is shown in Fig. 6.

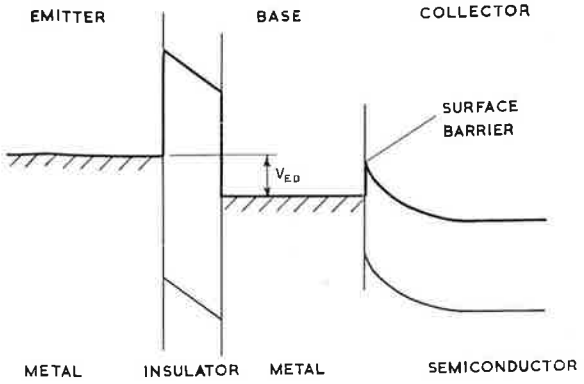

Fig. 6 — The metal-interface amplifier.

When the gold is biased negatively with respect to the aluminium by an amount V_{EB}, ~ a few tenths of a volt, electrons tunnel through the oxide and into the aluminium film. Some of these have sufficient energy at the far side of the aluminium layer to pass over the surface barrier at the aluminium-germanium interface, and these are collected. In operation, this device exhibits characteristics qualitatively similar to those of an n-p-n transistor, and power amplification of 20 db at 1 Kc has been observed. Current transfer ratios up to 0.9 have been observed for 100 A° aluminium. This implies a mean free path of ~ 1000 A°, which is in agreement with the value obtained photoelectrically for low energy electrons.

8. Collins, R. E. and Davies, L. W., unpublished.
9. Spitzer, W. G., Crowell, C. R. and Atalla, M. M., "Mean Free Path of Photoexcited Electrons in Au", *Phys. Rev. Letts.*, 8, Jan. 15, 1962, 57-58.
10. Crowell, C. R., Spitzer, W. G., Howarth, L. E. and La Bate, E. E., "Attenuation Length Measurements of Hot Electrons in Metal Films", *Phys. Rev.*, 127, Sept. 15, 1962, 2006-2015.
11. Quinn, J. J., "Range of Excited Electrons in Metals", *Phys. Rev.*, 126, May 15, 1962, 1453-1457.
12. Spratt, J. P., Schwarz, R. F., and Kane, W. M., "Hot Electrons in Metal Films: Injection and Collection", *Phys. Rev. Letts.*, 6, April 1, 1961, 341-342.
13. Schwarz, R. F. and Spratt, J. P., "A Tunnel Emission Device", *Proc. I.R.E.*, 50, April, 1962, 467.
14. Kahng, D., "A Hot Electron Transistor", *Proc. I.R.E.*, 50, June, 1962, 1534.
15. Hall, R. N., "Current Gain in Insulator-Metal Tunnel Triodes", *Solid State Elec.*, 3, Nov.-Dec., 1961, 320-322.
16. Lavine, J. M. and Iannini, A. A., "Experiments on the Metal-Interface Amplifier", *Solid State Elec.*, 5, Sept.-Oct., 1962, 273-283.
17. Geppert, D. V., "A Metal Base Transistor", *Proc. I.R.E.*, 50, June, 1962, 1527-1528.

It should be mentioned that some doubt exists[15, 16] as to the actual method of operation of this device, and there is evidence that the very thin aluminium film may have pinholes in it so that in places the gold emitter is in direct contact with the germanium. This would imply that at least part of the collected current was due to direct conduction between emitter and collector. However, some of the collected current is certainly due to the transport process discussed above[14].

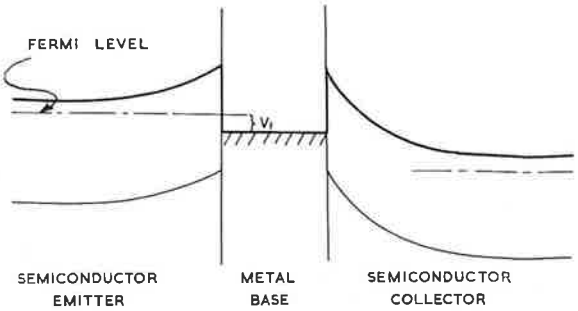

Fig. 7 — The metal base transistor.

The metal base transistor

An interesting new device[17], whose operation depends on the long mean free paths of low energy electrons in metals consists of a metal layer sandwiched between two layers of semiconductor. If one semiconductor layer is made negative with respect to the metal by an amount V_1, electrons will either tunnel through the potential barrier or pass over it (Schottky emission) and move into the metal (Fig. 7). The second semiconductor layer acts as a collector for those electrons which traverse the metal.

Although work is still in the preliminary stages, this device may be useful in high frequency applications, due to the very short transit times for electrons across the metal film.

Other tunneling effects

Electron tunneling is responsible for a number of other effects in solids.

(a) The fact that conduction is possible between terminals covered by a thin film of insulating material, e.g. grease, is due to electron tunneling through this insulating film.

(b) The apparent resistivity of very thin ($\gtrsim$ 30 A°) evaporated metal films is much higher than the bulk value. This is due to the fact that the films tend to form aggregates on the substrate which are separated from each other. Conduction in these films is thought[18] to be due to electron tunneling across the thin gaps separating these aggregates.

(c) As mentioned in 2.2, electron tunneling cannot take place unless there are vacant energy states on the far side of the barrier. The characteristics of several tunnel devices, including the Esaki diode, depend on this condition, and much useful knowledge about the band structure of semiconductors and superconductors has been obtained from the shape of the current-voltage characteristics of these devices.

Conclusion

Although the experimental work on electron tunneling is still in its early stages, several important new devices with potential application to electronic circuitry have emerged. A cold cathode which may give very high current densities has been constructed. Three terminal devices which exhibit power gain are being developed. These are particularly interesting for microcircuit applications, since they may be able to be prepared completely by vacuum evaporation. Perhaps the most fascinating aspect of tunneling work is the insight that it is giving us concerning the fundamental electronic transport processes which take place in solids.

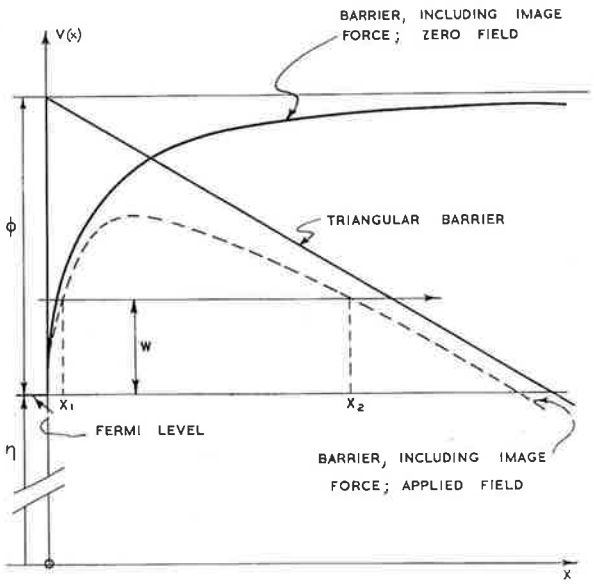

Fig. 8 — Metal-insulator potential barrier, effect of image force.

Acknowledgements

The author is pleased to acknowledge the valuable help and advice given by Dr. L. W. Davies, under whose guidance this work was carried out. He also wishes to thank W. M. Eades for assistance with the experimental work.

Appendix 1

Calculation of tunnel current

Electron tunneling probability can be evaluated exactly in only a few special cases, but approxi-

18. Neugebauer, C. A. and Webb, M. B., "Electrical Conduction Mechanism in Ultra Thin, Evaporated Metal Films", *J. Appl. Phys.*, 33, Jan., 1962, 74-82.

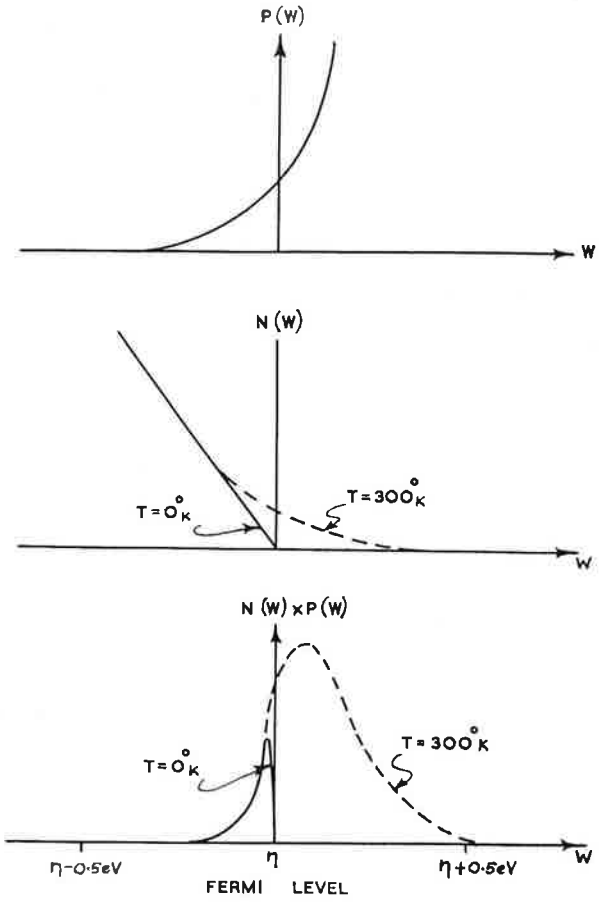

Fig. 9 — Calculation of tunnel current; (a) probability of tunneling; (b) number of electrons attempting to tunnel; (c) number of tunneled electrons—area under curve represents tunnel current.

mate formulae can be obtained using the WKB method if the potential energy varies by only a small amount in a distance comparable with the electron wavelength.

An exact calculation is possible in the case of a rectangular barrier[1] (Fig. 1(a)). In this case, the tunneling probability for an electron of energy W incident on a barrier of height V_0, and width a is

$$P(W) = 4/\{4\cosh^2\gamma a + (\gamma/\delta - \delta/\gamma)^2\sinh^2\gamma a\} \quad (6)$$

where

$$\delta\hbar = (2mW)^{\frac{1}{2}}$$

and

$$\gamma\hbar = [2m(V_0 - W)]^{\frac{1}{2}}.$$

For large γa, this approximates to

$$P(W) = 4\exp(-2\gamma a)/\{1 + (\gamma/\delta - \delta/\gamma)/4\} \quad (7)$$

For a triangular barrier of maximum height V_1, and thickness 1 at electron energy W (Fig. 1 (b)), the WKB method gives

$$P(W) = \exp(-4\beta 1/3) \quad (8)$$

where

$$\beta = [2m(V_1 - W)/\hbar^2]^{\frac{1}{2}}.$$

In both these expressions, the tunneling probability increases exponentially as the electron energy increases and as the barrier thickness decreases. Tunnel current is thus expected to be very sensitive to small changes in barrier shape which may be brought about for example, by an applied electric field. Because of the sensitivity of tunneling probability on barrier shape and size, the calculated current-voltage characteristics of a tunnel device may depend strongly on the particular model chosen for the energy barrier.

The simple band diagram for the metal-insulator-metal structure is shown in Fig. 3(b), (c) for zero bias and applied field respectively. The transition between metal and insulator is not expected to be sharp as shown, but exhibits image force rounding. This can be incorporated

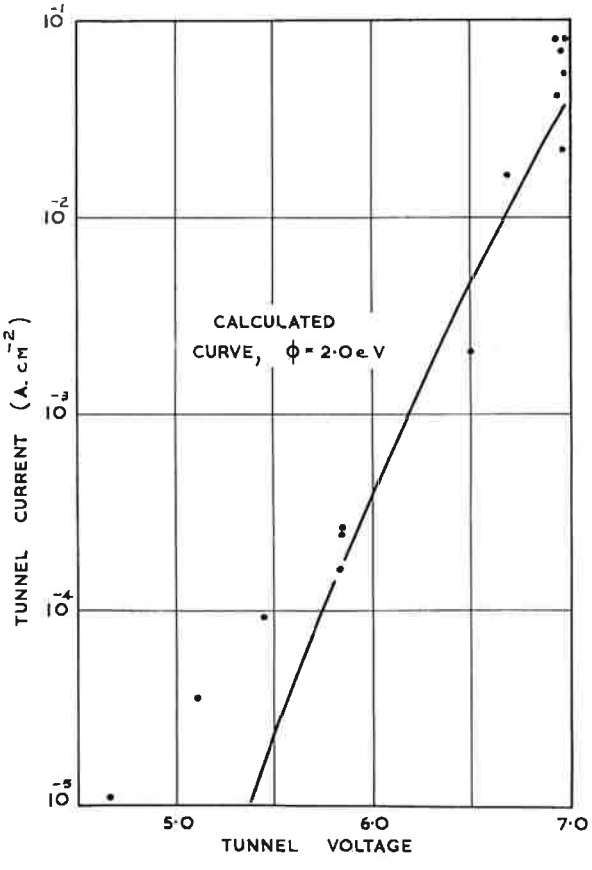

Fig. 10 — Current/voltage characteristics for tunnel structures, comparison of theory with experiment.

in the analysis by assuming[19] a barrier of shape

$$V(x) = \phi - e^2/(4x + e^2/\phi) \qquad (9)$$

where ϕ is the metal-insulator work function, and e is the electronic charge. With an applied electric field, F, the barrier shape becomes

$$V(x) = \phi - e^2/4x + e^2/\phi) - Fex \qquad (10)$$

These barriers are illustrated in Fig. 8. It is seen that higher fields will give rise to a lower and more narrow barrier, causing an increase in tunneling probability.

For an electron of energy W incident on such a barrier, (3) gives

$$P(W) = \exp(-2\alpha) \qquad (11)$$

where

$$\alpha = (2m/\hbar^2)^{\frac{1}{2}} \int_{x_2}^{x_1} [\phi - e^2/(4x + e^2/\phi) - Fex - W]^{\frac{1}{2}} dx.$$

This integral has not been solved analytically, and numerical methods must be used. It turns out that the exponent, -2α, in (11) varies approximately linearly with electron energy and with applied field.

In order to calculate the tunnel current through the barrier, it is necessary to find the number of electrons as a function of energy, incident on the barrier/unit area/unit energy range/sec. Fowler[20] gives the result that the number of electrons incident on a plane in a metal with energy component W normal to the plane is

$$N(W) = (4\pi mkT/h^3) \ln[1 + \exp\{(\eta - W)/kT\}] \qquad (12)$$

electrons/unit area/unit energy interval/sec., where η is the energy of the Fermi level, K is Boltzmann's constant, and T is the absolute temperature.

The total current through the barrier is given by (4). Here the component in the reverse direction is negligible, and so the tunnel current density is

$$j(F) = \int_0^\infty N(W) \exp[-2\alpha(F, W)] dW. \qquad (13)$$

The integration must be performed numerically since α is not analytic. Fig. 9 (a), (b) illustrate how the factors P(W) and N(W) vary with electron energy for a given electric field. The product of these factors is shown in Fig. 9 (c) and it is seen that most of the tunneled electrons originate from energy levels within a few tenths of an electron volt of the Fermi level. Fig. 9 (c) also shows the effect of temperature on the tunnel current. Tunneling probability is independent of temperature and all the variation in tunnel current arises from changes in the N(W) term.

Experimental results[8, 20] show good agreement over 3 orders of magnitude with the results of this analysis. Fig. 10 shows the experimental and calculated current-voltage characteristics for a 100 A° insulating aluminium oxide film, assuming $\phi = 2.0$ev. Qualitative agreement between theory and experiment[21] is obtained for the effect of temperature variation on the tunnel current.

Reprinted from Proceedings of the I.R.E. Aust., by kind permission of the Institution.

19. Seitz, F., "The Modern Theory of Solids", McGraw-Hill, 1940, 163.
20. Fowler, R. H., "Statistical Mechanics", Cambridge, 1936, 342.
21. Advani, G. T., Gottlung, J. G. and Osman, M. S., "Thin Film Triode Research", *Proc. I.R.E.*, 50, June, 1962, 1530-1531.

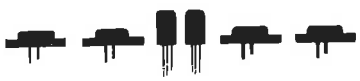

A Series on Tunnel Diodes

5: MICROWAVE AMPLIFIERS

TUNNEL-DIODE amplifiers can be useful as low-noise rf amplifiers in the front end of microwave receivers.[23] Although lower noise figures can be obtained with masers and parametric amplifiers, tunnel-diode amplifiers are dc-activated, i.e., they do not require ac pumping. As a result, tunnel-diode amplifiers are most desirable for low-noise applications in which the primary considerations are low cost, small size and weight, and low power drain.

Tunnel-diode amplifiers are inherently broadband devices because a properly biased tunnel diode has a negative input resistance at all frequencies from dc to the resistive cutoff frequency. When this negative input resistance is combined with a suitable coupling network, a circuit can be designed having an over-all positive input impedance that provides amplification or power gain. Because of this wideband negative-resistance characteristic, bandwidths in excess of an octave can be readily obtained with tunnel-diode amplifiers.[24, 25] Masers and parametric amplifiers require extensive development before bandwidths in excess of ten per cent can be achieved. The wideband negative resistance, however, makes stabilization of tunnel-diode amplifiers an important developmental problem.

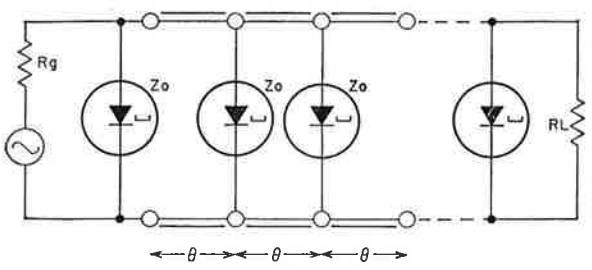

Fig. 73—Travelling-wave tunnel diode amplifier.

Microwave tunnel-diode amplifiers are applicable to various types of communications, radar, and countermeasures systems. In addition, the size and weight of these amplifiers is attractive for tactical electronic equipment. Because of the low power drain of tunnel-diode amplifiers, they should prove quite useful in space applications such as communication satellites. The relatively low cost of tunnel-diode amplifiers also makes them strong contenders in line-of-sight radio-relay systems and phased-array radars.

Types of Amplifier Circuit

All tunnel-diode amplifier circuits employ diodes biased in the negative-resistance region. Direct-coupled tunnel-diode amplifiers are difficult to stabilize and are rarely used at microwave frequencies. However, various types[26] of circuit techniques can be used to achieve a positive input impedance for tunnel-diode amplifiers. The advantages and disadvantages of several methods are discussed below:

Travelling-Wave Tunnel-Diode Amplifiers. In this type of circuit, several tunnel diodes are periodically spaced along a transmission line, as shown in Fig. 73. Travelling-wave tunnel-diode amplifiers were originally developed to achieve octave-bandwidth amplification. However, because very broadband tunnel-diode amplifiers can be readily realized by other circuit techniques, travelling-wave tunnel-diode amplifiers have not been particularly popular. Nevertheless, some research on this type of circuit is still being done.

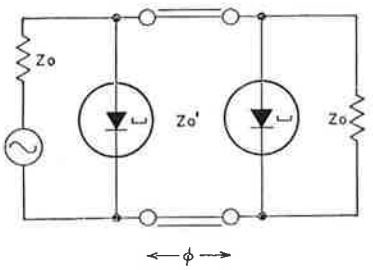

Fig. 74—Quarter-wave-coupled tunnel diode amplifier.

Quarter-Wave Coupled Tunnel-Diode Amplifiers. In this method, two tunnel diodes are separated by a length of transmission line that is $\lambda/4$ long at the design-centre frequency of the amplifier. An example of this circuit is shown in Fig. 74. This circuit requires a matched pair of tunnel diodes and has not been used extensively at microwave frequencies.

Hybrid-Coupled Tunnel-Diode Amplifiers. This technique uses a matched pair of tunnel diodes coupled to conjugate ports of a hybrid or 3-db directional coupler, as shown in Fig. 75. A hybrid coupler is a four-port network that can deliver half the power incident upon port No. 1 to ports Nos. 2 and 3. The fourth port is isolated from the input port by 20 to 40 db. If two signals are delivered to ports Nos. 2 and 3, the hybrid can also combine these signals. In a tunnel-diode amplifier, the hybrid used must provide power division with quadrature phase between outputs. Hybrids such as the "magic-T" or "rat-race" are not applicable unless an external quarter-wave coupling line is used for one of the tunnel diodes. This requirement makes the amplifier more frequency-sensitive and, as a result, is generally not desirable.

Circulator-Coupled Tunnel-Diode Amplifiers. The circulator-coupled amplifier is the preferred approach for most tunnel-diode applications at microwave frequencies. This type of circuit uses a ferrite circulator and only one tunnel diode, as shown in Fig. 76. The ferrite circulator is a non-reciprocal device having low insertion loss (in the order of a few tenths of a db) in the forward direction and a high insertion loss (about 20 db) in the reverse direction. Fig. 77 shows another type of circulator-coupled amplifier which uses four ports. This method offers better amplifier stability than the three-port circuit.

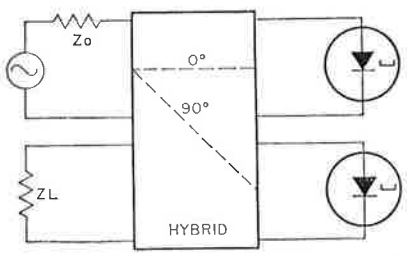

Fig. 75—Hybrid-coupled tunnel diode amplifier.

Gain Bandwidth

The circuit parameters of tunnel-diode amplifiers can be combined to form several convenient design values:[25]

$$\omega_o^2 = \frac{1}{LC_j} \qquad \eta = \frac{Z_o}{|R_j|} \qquad Z^2 = \frac{L}{C_j}$$
$$\beta^2 = \left(\frac{\omega}{\omega_o}\right)^2 \qquad \gamma = \frac{Z}{|R_j|} \qquad \theta = \frac{R_s}{|R_j|} \qquad (53)$$

where Z_o is the source-load impedance of the quarter-wave-coupled, hybrid-coupled, or circulator-coupled tunnel-diode amplifiers; L is the overall series inductance, including both tunnel-diode lead inductance and external wiring; and ω is the angular frequency ($2\pi \times$ the signal frequency f_s).

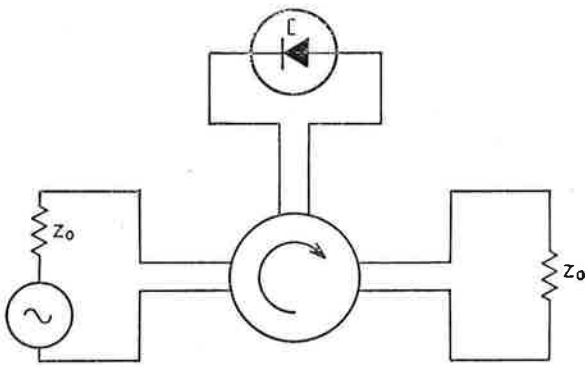

Fig. 76—Circulator-coupled tunnel diode amplifier.

If an ideal hybrid having source-load impedance equal to Z_o is assumed, the gain G for a hybrid-coupled tunnel-diode amplifier[27] is given by

$$G = 10 \log |\Gamma|^2 \qquad (54)$$

where $|\Gamma|$ is the magnitude of the voltage-reflection coefficient of the tunnel-diode network.

By substitution of the parameters of the tunnel-diode network for $|\Gamma|^2$, Eq. (54) can be rewritten as follows:

$$G = 10 \log \left[\frac{(\beta^2 - 1 - \eta + \theta)^2 + \beta^2 (\gamma + \eta/\gamma - \theta/\gamma)^2}{(\beta^2 - 1 - \eta + \theta)^2 + \beta^2 (\gamma - \eta/\gamma - \theta/\gamma)^2}\right] \text{ db} \qquad (55)$$

If the dissipative resistance of the tunnel diode is neglected (i.e., $\theta = 0$), the expression for gain becomes

$$G = 10 \log \left[\frac{(\beta^2 - 1 - \eta)^2 + \beta^2 (\gamma + \eta/\gamma)^2}{(\beta^2 - 1 - \eta)^2 + \beta^2 (\gamma - \eta/\gamma)^2}\right] \text{ db} \qquad (56)$$

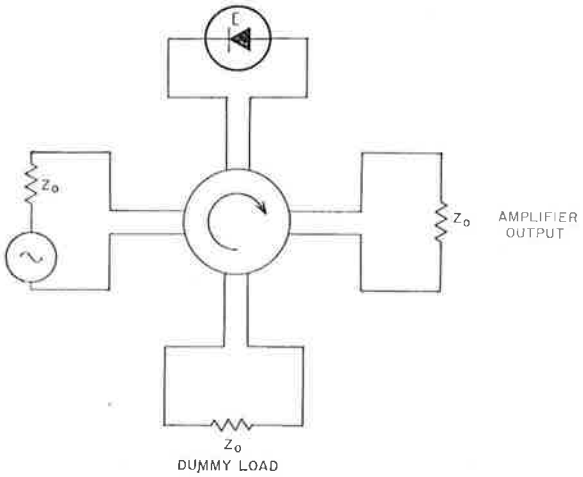

Fig. 77—Circulator-coupled tunnel diode amplifier having a four-port circulator.

This expression is for a low-pass prototype circuit in which the lead inductance of the diode acts as a peaking coil. This effect can be seen in Fig. 78, which shows the gain of tunnel-diode amplifiers as a function of the normalized frequency for various degrees of peaking, i.e., different values of the parameter

$$\gamma = \frac{Z}{|R_j|} = \sqrt{\frac{LC_j}{|R_j|}}$$

Larger values of this parameter are used for higher low-frequency values of gain.

If both the lead inductance and junction capacitance of the tunnel diode are neglected, the amplifier gain at dc is given by

$$G = 20 \log \left[\frac{1+\eta}{1-\eta}\right] \text{ db} \qquad (57)$$

Typical values of η for practical tunnel-diode amplifiers range from 0.5 to about 0.8.

If the spreading resistance and the lead inductance are neglected, the gain of the tunnel-diode amplifier is given by

$$G = 10 \log \left[\frac{(1+\eta)^2 + W^2}{(1-\eta)^2 + W^2}\right] \text{ db} \qquad (58)$$

where $W = 2\pi f C_j Z_o$. For a high-gain amplifier (i.e., the value of G approaches ∞), the gain-bandwidth product $BG^{1/2}$ is given by

$$BG^{1/2} = \frac{1}{\pi |R_j| C_j} \qquad (59)$$

The above gain equations are equally applicable for a circulator-coupled tunnel diode using an ideal ferrite circulator.

Noise Figure

In general, it is convenient to express the noise characteristics of a two-port tunnel-diode amplifier in terms of the noise figure.[28, 29, 30] This term is described quantitively as the signal-to-noise ratio at the amplifier input divided by the signal-to-noise ratio at the amplifier output. The noise figure NF for hybrid-coupled or circulator-coupled tunnel-diode amplifiers using ideal hybrids or circulators is given by

$$NF = 1 + \frac{4}{G}\left[\frac{20\, I_o Z_o}{(1-\eta-\theta-\beta^2)^2 + \beta^2(\gamma-\eta/\gamma-\theta/\gamma)^2}\right] + \frac{4}{G}\left\{\frac{\theta/\eta}{\left[1+\frac{\theta}{\eta}-\frac{1/\eta}{1+\beta^2/\gamma^2}\right]^2 + \beta^2\left[\frac{\gamma}{\eta}-\frac{1/\gamma\eta}{1+\beta^2/\gamma^2}\right]^2}\right\} \qquad (60a)$$

where NF is the noise figure as a power ratio and I_o is the static current at the operating point of the tunnel diode. If the inductance is omitted, this equation can be reduced to the following expression:

$$NF = \frac{1}{G} + \left[1-\frac{1}{G}\right]\left[\frac{1 + 20\, I_o |R_j|}{(1 - R_s/|R_j|)\ (1 - f_s/f_{ro})^2}\right] \qquad (60b)$$

where f_{ro} is the resistive cutoff frequency.

For a perfect amplifier, the noise figure is equal to unity. For practical amplifiers, the component of the noise figure greater than unity is

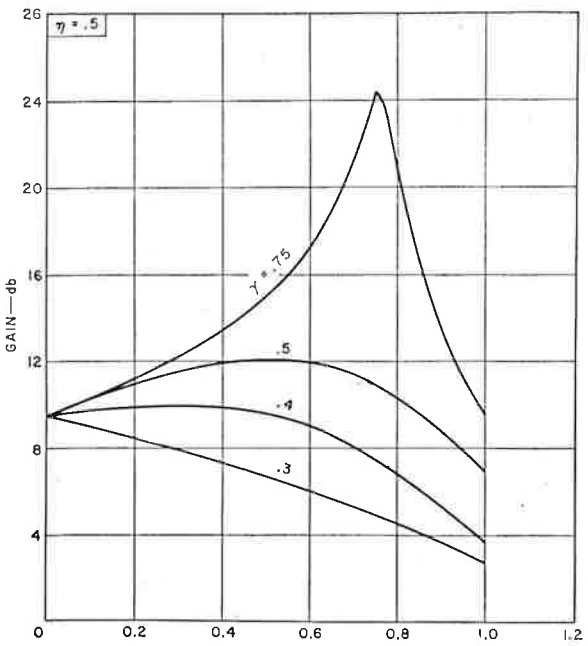

Fig. 78—Gain as a function of normalised frequency.

called the excess noise. The second term in Eq. (60a) is the excess noise caused by shot noise; the third term is excess noise caused by thermal noise in the dissipative resistance of the tunnel diode.

The resistive cutoff frequency of the tunnel diode is given by

$$f_{ro} = \frac{1}{2\pi \mid R_j \mid C_j}\sqrt{\frac{R_j}{R_s} - 1} = \frac{\gamma\omega_o}{2\pi}\sqrt{\frac{1}{\theta} - 1} \quad (61)$$

For frequencies less than $f_{ro}/3$, the excess noise in the series resistance can usually be neglected. If both β and θ are equal to zero in Eq. (60a) and if the high-gain approximations of $Z_o = \mid R_j \mid$ and G approximately equal to $4/(1 - \eta)^2$ are used, the equation for noise figure reduces to

$$NF = 1 + 20\, I_o \mid R_j \mid \quad (62)$$

The factor $(20\, I_o \mid R_j \mid)$ is a function of temperature and is sometimes called the **noise constant** of the tunnel diode. For germanium tunnel diodes, the noise constant is usually equal to at least 1.1; as a result, the minimum noise figure is about 3.6 db. Lower room-temperature noise figures can be achieved by use of gallium antimonide tunnel diodes; however, these devices are extremely temperature-sensitive, and the power required to regulate the temperature of a gallium antimonide tunnel-diode amplifier makes such an amplifier much less attractive for many applications.

Maximum gain in a tunnel-diode amplifier occurs when the tunnel diode is biased at the point of inflection on its static current-voltage characteristic curve. Minimum noise figure occurs at a somewhat larger bias-voltage point. As a result, amplifier bias is usually adjusted experimentally to minimize the noise figure.

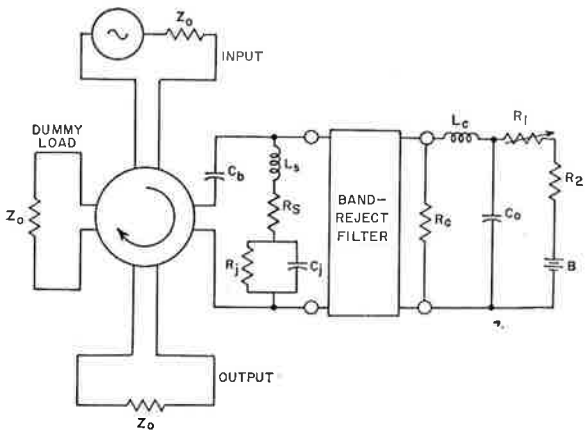

Fig. 79—Typical circuit of a stable microwave tunnel diode amplifier.

Eq. (62) can also be used as an approximate estimate of the noise figures of other tunnel-diode amplifiers, such as quarter-wave-coupled amplifiers.

Stability

The low-pass prototype tunnel-diode network displays a negative resistance at its external coupling network over a broad range of frequencies outside the useful bandwidth of the amplifier. Consequently, parasitic oscillations (relaxation and/or sinusoidal) may occur if special design precautions are not observed. The first problem that must be investigated is whether or not the tunnel diode being considered can be employed in a stable amplifier.[31] For lossy tunnel diodes, the following practical conditions are sufficient for stability:

$$\frac{R_s}{R_j} = \theta \leqq 0{\cdot}5$$
$$\frac{L_s}{R_j^2 C_j} = \gamma^2 \leqq 1{\cdot}0 \quad (63)$$

Depending upon the circuitry used to inject dc bias into the tunnel diode, spurious relaxation oscillation can occur. Typical tunnel-diode circuits have been analyzed from the standpoint of freedom from these relaxation oscillations.[26, 31] Spurious rf oscillations are avoided if the tunnel-diode network presents a positive input impedance to the external coupling networks (i.e., hybrid or circulator) at all frequencies outside the desired amplifier bandwidth that are less than the resistive cutoff frequency of the diode. Amplifier bandwidths are restricted to the passband of the hybrid or circulator.

The network shown in Fig. 79 is recommended for unconditionally stable microwave tunnel-diode amplifiers, i.e., amplifiers which do not oscillate because of changes in source load impedance or dc bias. A band-reject filter is used between the tunnel-diode network and the dc-bias source. The resistor R_c is much less than the absolute value of the negative resistance. When the band-reject filter is in its "stopband", the resistor R_c does not act as a load in the tunnel-diode network. At this point, a negative resistance is presented to the circulator and gain is realized. When the band-reject filter is in its passband (i.e., off resonance), R_c acts as a load in the tunnel-diode network. In this case, a positive resistance is presented to the circulator so that no gain and/or spurious oscillations occur.

The bandpass of a narrow-band tunnel-diode amplifier can be shaped by the band-reject filter. The band-reject filter must be free of spurious stopbands, and the resistor R_c must maintain its characteristics at all microwave frequencies below the resistive cutoff frequency of the tunnel diode.

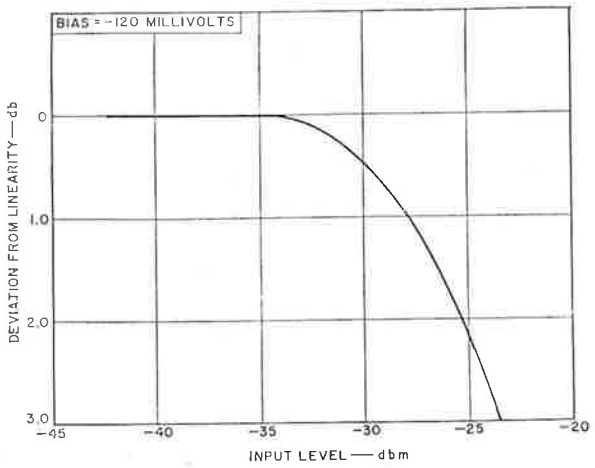

Fig. 80—Gain as a function of frequency for a hybrid-coupled tunnel diode amplifier.

For this reason, tunnel-diode cutoff frequencies should be about three to four times the highest value of the amplifier operating frequency. Use of lower cutoff frequencies significantly degrades amplifier noise figure; use of higher cutoff makes stabilization more difficult.

Stable operation within the passband of the amplifier depends upon the type of coupling network used and the voltage-reflection coefficient of the input, output, and dummy loads. For the hybrid-coupled tunnel-diode amplifier having an ideal hybrid, the stability threshold occurs when the following condition exists:

$$| \Gamma_g | \quad | \Gamma_L | \quad G = 1{\cdot}0 \qquad (64)$$

where $| \Gamma_g |$ is the magnitude of the voltage-reflection coefficient of the source and $| \Gamma_L |$ is the magnitude of the voltage-reflection coefficient of the load.

For a tunnel-diode amplifier using a three-port ideal circulator, the stability threshold occurs when the following condition exists:

$$| \Gamma_g | \quad | \Gamma_L | \quad G^{1/2} = 1{\cdot}0 \qquad (65)$$

For a tunnel-diode amplifier using a four-port ideal circulator, the stability threshold occurs when the following condition exists:

$$| \Gamma_g | \quad | \Gamma_L | \quad | \Gamma_o | \quad G^{1/2} = 1{\cdot}0 \qquad (66)$$

where $| \Gamma_o |$ is the magnitude of the voltage-reflection coefficient of the dummy load.

The most favorable conditions of passband stability can usually be achieved by use of a four-port circulator because the value of $| \Gamma_o |$ to which is equal to or less than 0.048 (i.e., when the VSWR is equal to or less than 1.10) can usually be obtained readily.

(In the case of mismatched source-load impedances, Eqs. (54) through (60) and (62) must be modified for the calculation of amplifier gain and noise figure.)

Dynamic Range

The dynamic range of a tunnel-diode amplifier is the range of input signal levels that can be accommodated by the amplifier. The lower limit of the dynamic range of a tunnel-diode amplifier is determined by noise considerations; the upper limit is limited by the large-signal saturation phenomena of the tunnel diode as a device. (The upper limit usually extends to the 3-db gain compression point.) The amplifier gain, the nature of the input signals, and the tunnel diode being used determine what large signals can cause in significant intermodulation, crossmodulation, and harmonic outputs.[32, 33] For typical microwave low-noise tunnel-diode amplifiers, saturation occurs at signal-input levels between —25 and —50 dbm. In general, saturation occurs at somewhat lower levels in tunnel-diode amplifiers than in tunnel-diode converters or parametric amplifiers and converters.

Measured Results

Fig. 80 shows the frequency response for a typical broadband hybrid-coupled tunnel-diode amplifier. This circuit does not use a band-reject filter for narrow-banding. Germanium tunnel diodes having peak currents of about one milliampere were used with this unit, and noise figures of 4.0 to 4.5 db were obtained. Hybrid-coupled uhf tunnel-diode amplifiers have been developed having useful gain over a five-to-one frequency range. Various circulator-coupled narrow-band amplifiers have also been developed. A typical gain-saturation characteristic for a practical tunnel-diode amplifier is shown in Fig. 81.

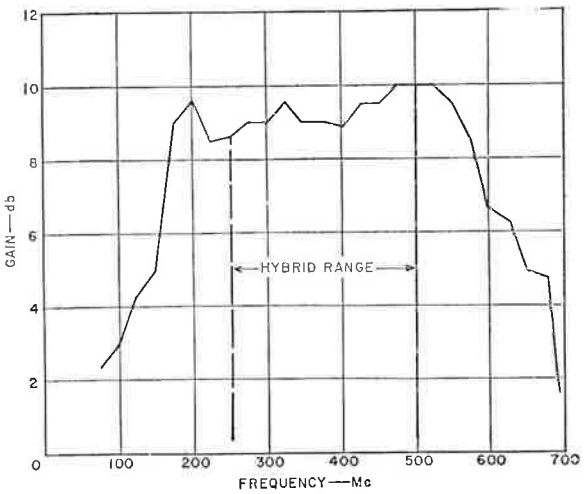

Fig. 81—Typical gain-saturation characteristic of tunnel diode amplifier.

References

23. H. S. Sommers, "Tunnel Diodes as High-Frequency Devices", *Proc. IRE,* Vol. 47, pp. 1201-1206, July, 1959.
24. J. J. Sie, "Absolutely Stable Hybrid-Coupled Tunnel-Diode Amplifier", *Proc. IRE,* Vol. 48, p. 1321, July, 1960, plus correction p. 1783, August, 1960.
25. H. Boyet, B. Fleri and R. M. Kurzrok, "Broadband Hybrid-Coupled Tunnel-Diode Amplifier in the UHF Region", *Proc. IRE,* Vol. 50, p. 1527, June, 1962.
26. M. E. Hines, "High-Frequency Negative-Resistance Circuit Principles for Esaki-Diode Applications", *BSTJ,* Vol. 39, pp. 477-513, May, 1960.
27. R. M. Kurzrok, "Bandwidth of Hybrid-Coupled Tunnel-Diode Amplifier", *Proc. IRE,* Vol. 50, pp. 226-227, February, 1962, plus correction p. 466, April, 1962.
28. K. K. N. Chang, "The Optimum Noise Performance of Tunnel-Diode Amplifiers", *Proc. IRE,* Vol. 48, pp. 107-108, January, 1960.
29. L. S. Nergaard, Comments on "Shot Noise in Tunnel-Diode Amplifiers", plus reply by J. J. Tiemann, *Proc. IRE,* Vol. 49, pp. 622-623, March, 1961.
30. E. O. Nielsen, "Noise Performance of Tunnel Diodes", *Proc. IRE,* Vol. 48, pp. 1903-1904, November, 1960.
31. H. Boyet, B. Fleri and C. A. Renton, "Stability Criteria for a Tunnel-Diode Amplifier", *Proc. IRE,* Vol. 49, p. 1937, December, 1961.
32. R. M. Kurzrok and A. Newton, "Non-Linear Distortion in Tunnel-Diode Amplifiers", *Proc. IRE,* Vol. 50, p. 1853, August, 1962.
33. R. M. Kurzrok, "AM to PM Conversion in Tunnel-Diode Amplifiers", *Proc. IEEE,* Vol. 51, pp. 377-378, February, 1963.

NOTICE RE SUBSCRIPTIONS

Readers and intending subscribers are reminded that the subscription rate for this magazine is now £1 (£1/5/- foreign) for 12 issues, and that subscriptions are accepted for multiples of 12 issues if required. Delivery commences with the first issue after receipt of order. Back copies for the current year and previous year may be ordered separately if required; the rate for back copies is 2/6 per copy, post free.

Simple binders intended to hold 12 copies are available at 2/6 each post free, whilst existing stocks last.

Changes of address require one month to become effective, and normally operate on the first issue mailed after receipt of advice. Subscribers are particularly reminded that requests for changes of address should include both the old and the new address; this ensures speedy handling, and protects other subscribers of the same name.

New address stencils now coming into use will carry information regarding the duration of the subscription, allowing readers to check for themselves when their subscriptions are due to terminate. These stencils will be used progressively as renewals are made. The stencil carries a code consisting of two numerals and a letter. The two numerals are the last two figures of the expiry year, whilst the letter shows the last monthly issue due. The letters commence with "a" for January, and go through, omitting "i" and "l", to "n" for December. Thus, for example, code 64j indicates the last copy due to be that for September, 1964. At this date, only a small number of readers have these coded stencils, but it is expected that all will have them shortly.

6: MICROWAVE CONVERTERS

Practically all existing low-noise uhf and microwave receivers make use of the heterodyne principle, i.e., the frequency of the received signal is shifted before high amplification takes place. For frequencies above a few hundred megacycles, crystal diodes have been almost universally used in the frequency converters of such receivers. However, the best uhf crystal converters have conversion losses of 3 to 4 db and noise figures of 4 to 5 db; at microwave frequencies, both conversion losses and noise figures are somewhat higher. Until the recent advent of very-low noise preamplifiers such as masers, parametric amplifiers, and travelling-wave valves, crystal frequency converters were generally placed directly at the input of the receiver. In more recent designs, a low-noise preamplifier has been placed ahead of the crystal to provide very low receiver noise figures.

There is little likelihood that the noise figure of crystal mixers can be significantly improved by further research. Crystal diodes, which are passive devices, must have some conversion loss, and their noise figure must always equal or exceed this loss. However, microwave diodes with a negative-resistance region (tunnel diodes), exhibit active properties even at millimetre-wave frequencies.[34]

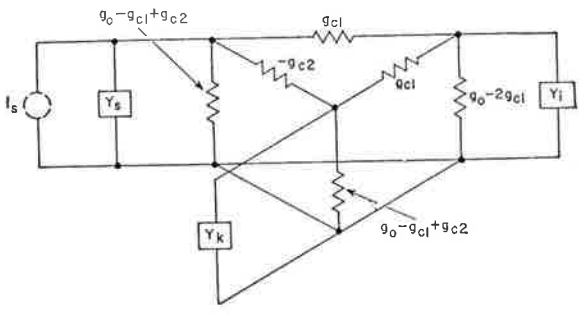

Fig. 82—Equivalent linear three-port frequency-translation network for tunnel diode frequency converter.

Tunnel-diode frequency converters have lower conversion loss, lower noise figures, larger dynamic range, and greater resistance to burn-out than crystal-diode converters; their use could eliminate the need for preamplifiers in many applications.

Equivalent Circuit

In a tunnel-diode frequency converter, an input signal of frequency f_s and a local-oscillator signal of frequency f_o are impressed across the nonlinear conductance of the diode. In general, a complete set of side band frequencies is produced, i.e., all frequencies $f_{m,n} = mf_s + nf_o$ (m and n take on all integral values) are present. However, in most practical converters, significant power flow takes place only at the input-signal frequency f_s, the oscillator-frequency f_o, the intermediate frequency $f_i = |f_s - f_o|$, and the image frequency $f_k = |2f_o - f_s|$. In this case, the converter can be represented by the linear three-port frequency-translation network shown in Fig. 82, provided that the amplitude of the sinusoidal local-oscillator voltage across the nonlinear conductance is much greater than the sum of the amplitudes of the voltages at signal, intermediate, and image frequencies.[35]

In Fig. 82, Y_s is the total admittance at the signal frequency connected across the nonlinear conductance; similarly, Y_k and Y_i are, respectively, the total image- and intermediate-frequency

admittances. The quantity g_o is the average value of the nonlinear conductance driven by the sinusoidal local oscillator, g_{c1} is the fundamental conversion conductance, and g_{c2} is the second-harmonic conversion conductance. (The equivalent circuit of Fig. 82 can also be used to calculate the gain of a converter in which the signal mixes with the nth harmonic of the local oscillator ($f_s = 2nf_o - f_k$). In this case, g_{c1} and g_{c2} must be replaced by g_{cn} and g_{c2n}, respectively. The values for g_o, g_c, and g_{c2} are evaluated for germanium tunnel diodes in reference 35.

In practical positive nonlinear-conductance mixers, the following inequalities must always be satisfied:[36]

$$g_o > O, g_o > | g_{c1} | , g_o > | g_{o2} | \qquad (67)$$

However, these restrictions do not apply to tunnel-diode converters because tunnel diodes exhibit a negative conductance over part of their current-voltage characteristic.

Conversion Gain

Expressions for the conversion gain (i.e., the ratio of if output power to the available signal power) can also be derived from the equivalent circuit shown in Fig. 82. If, for simplicity, it is assumed that Y_s, Y_k, and Y_i are pure conductances equal to the internal conductance of the generator g_g, the image conductance g_k, and the load conductance g_i, respectively, then the conversion gain K can be expressed as follows:

$$K = \frac{4g_i g_g M^2}{(g_g + g_{in})^2} \qquad (68)$$

where

$$M = \frac{g_{c1}(g_o + g_k - g_{c2})}{(g_o + g_k)(g_o + g_i) - g_{c1}^2}$$

and where g_{in}, the input conductance, is given by

$$g_{in} = \frac{g_{c1}^2(2g_{c2} - 2g_o - g_k) - (g_o + g_i)(g_{c2}^2 - g_o^2 - g_o g_k)}{(g_o + g_k)(g_o + g_i) - g_{c1}^2}$$

Passive converters must have conversion loss, as can be shown by the insertion of Eq. (67) into Eq. (68). Tunnel-diode converters, on the other hand, may have conversion gain when any one of the inequalities in Eq. (67) is reversed. This conversion gain can be made arbitrarily large, and approaches infinity as $-g_{in}$ approaches g_g.

Bandwidth

The conversion gain of a nonlinear-conductance frequency converter containing no reactances is independent of frequency. Tunnel diodes, however, contain parasitic capacitances and inductances; as a result, the gain of tunnel-diode frequency converters is frequency-dependent. With available tunnel diodes, the effect of these reactances is usually negligible at conventional intermediate frequencies (30 megacycles or less), but must be taken into account at uhf and microwave frequencies.

An approximate equivalent ac circuit for an encapsulated tunnel diode consists of three elements connected in series: an inductance L_s, a resistance R_s, and a voltage-dependent resistance R_j (v) (1/g) shunted by a voltage-dependent capacitance C_j (v). L_s results mainly from the inductance of the housing; R_s is the resistance of the ohmic contact, the base, and the internal leads of the package, and is a function of frequency due to skin effect. C_j (v) is the junction capacitance*, and R_j (v) is the total ac resistance of the junction, where v is the voltage across R_j and C_j. The bandwidth of the converter can be calculated in a straightforward fashion if R_s, L_s, and C_j are incorporated into the admittances Y_s, Y_k, and Y_i of the equivalent circuit of Fig. 82, and the equivalent circuit is then used to calculate gain as a function of frequency. This circuit is shown in Fig. 83.

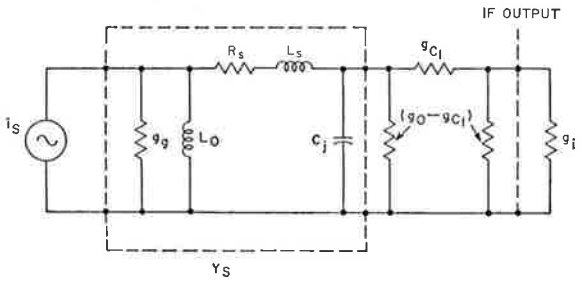

Fig. 83—Equivalent circuit used for bandwidth calculation.

Spurious Oscillations

A tunnel diode biased in its negative-resistance region, or driven into this region by an applied local-oscillator voltage, can generate rf oscillations. In autodyne frequency converters, advantage is taken of the self-oscillations of the tunnel diode to supply the local-oscillator drive. In converters with external local oscillators, however, self-oscillation must be prevented because these oscillations cause spurious responses and instabilities, and usually increase the noise of the converter.

Converter circuits that do not oscillate at any bias voltage without local-oscillator drive are also

* The variation of C_j with voltage may be approximated for voltages less than the valley voltage by $C_j(v) \approx K(\Phi - v)^{-1/2}$ where K and Φ are constants. For germanium, Φ is approximately 0.6 volt. For a diode driven by a sinusoidal local oscillator, the average value of C_j is approximately equal to the value of C at the bias point.

stable at any bias when driven by the local oscillator. This type of converter circuit must use "stable" diodes, i.e., diodes for which the following inequality exists:[37]

$$L_s < 3R_j^2C_j \qquad (69)$$

For stable diodes, the limits on the maximum usable peak current I_p and the minimum time constant R_jC_j are set by Eq. (69); for unstable diodes, these parameters are limited only by semiconductor fabrication techniques. Consequently, unstable tunnel diodes are often useful in high-power or high-frequency converters. (The power-handling capability of a diode is, in general, proportional to I_p. Also, the cutoff frequency, i.e., the frequency above which the real part of the diode impedance becomes positive, is proportional to $(|R_j|C_j)^{-1}$. It has been found experimentally that spurious oscillations in converters using unstable tunnel diodes can be prevented by use of a large local-oscillator drive (V_o is more than 0.1 volt). This procedure is most effective if the local-oscillator frequency is close to the self-oscillation frequency of the converter.

Noise Figure

The noise figure NF of a nonlinear-conductance converter with short-circuited image impedance ($Y_k = \infty$) and with real input admittance can be written as follows:

$$NF = 1 + \frac{T}{T_o}\left(\frac{G_o(g_o + g_g)^2}{g_g g_{c1}^2} - \frac{2(g_o + g_g)G_{c1}}{g_g g_{c1}} + \frac{G_o}{g_g}\right) \qquad (70)$$

where T is the ambient temperature and T_o is the standard reference temperature of G_o and G_{c1} are the short-noise conductances of the diode. (G_o and G_{c1} are evaluated for germanium tunnel diodes in reference 35.) In the derivation of Eq. (70), it was assumed that the noise currents at the signal and intermediate frequencies generated by the pumped nonlinear conductance are fully correlated. Also, in accordance with the IRE definition[38], the noise figure is written in terms of available noise output power, and does not take into account any noise contributions from the if load.

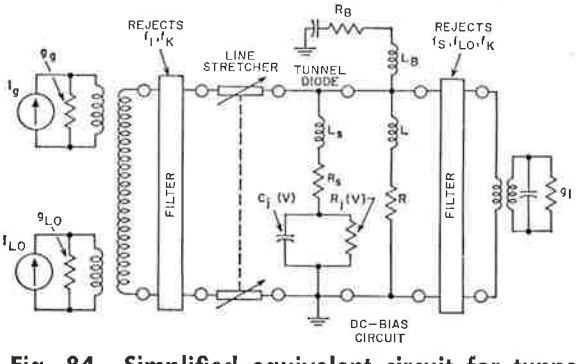

Fig. 84—Simplified equivalent circuit for tunnel diode frequency converter having image rejection.

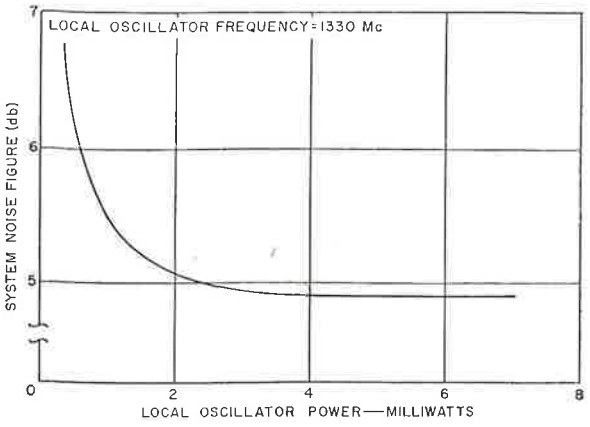

Fig. 85—System noise figure as a function of local oscillator power for a balanced converter (noise figure of if amplifier equals 17.5 db).

The noise figure of a tunnel-diode frequency converter, like the noise figure of a passive converter, must always exceed unity. However, the minimum noise figure that can be achieved with a tunnel-diode converter is lower than the minimum noise figure of a passive converter because the conductances g_o and g_{c1} in a tunnel-diode converter are not restricted by Eq. (67).

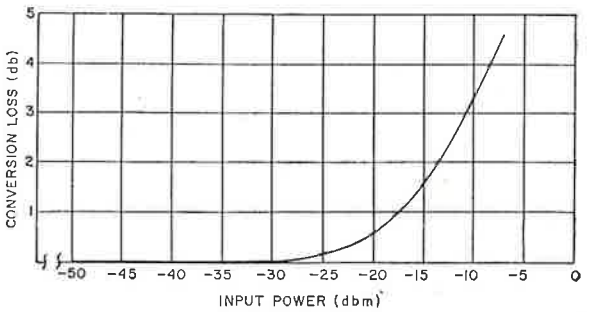

Fig. 86—Conversion loss as a function of input power for a uhf tunnel diode frequency converter.

Experimental Converters

Fig. 84 shows a simplified equivalent circuit for a converter with image rejection. Except for the dc bias circuit, which is designed to prevent spurious oscillations while the diode swings through the negative-resistance region, the equivalent circuit is similar to conventional passive frequency converters. The sizes of actual converters are generally comparable to those of miniaturized passive frequency converters.

Local-Oscillator Frequency (Mc)	Signal Frequency (Mc)	Double-Sideband System Noise Figure (db)	Single-Sideband System Noise Frequency (Image Rejection, 10db)
482	512		5
780		3·9	
1340		4·3	
1340	1370		5·5
2000		5·5	
10400		6·8	

Table 4—Measured system noise figures.

The conversion gain of a tunnel-diode frequency converter can be adjusted to any convenient value by suitable choice of diode and circuit parameters, bias voltage, and local-oscillator drive. Converters having conversion gain of more than a few db are very sensitive to variations in input impedance. On the other hand, converters having zero conversion gain, or conversion loss, are generally stable with input VSWR's exceeding 10:1 varied through all phases. Furthermore, the lowest system noise figures (when a 30-megacycle if amplifier having a 1.7 db noise figure is used) are obtained with converters having conversion losses in the neighbourhood of zero db.

The system noise figure of a balanced L-band converter is shown in Fig. 85 as a function of local-oscillator power. The noise figure varies little for local-oscillator power in the range from about 2 to 7 milliwatts. The use of this relatively high pump power results in a large dynamic range. (Saturation effects occur only when the signal voltage across the diode becomes a significant fraction of the local-oscillator voltage.) Fig. 26 shows the conversion loss of a typical single-ended converter as a function of input power. The conversion loss is increased by 3 db at an input of about 0.1 milliwatt. (In some more recent experiments with balanced mixers, 3-db gain compression occurred at a signal level of about one millivolt. The bandwidth of these converters was 250 megacycles centred at a frequency of 1270 megacycles.) The sensitivity of this converter to inputs at unwanted frequencies is comparable to that of crystal-diode converters. For one-per-cent intermodulation distortion, the power in the unwanted signal is about —30 dbm.

Burnout, i.e., detectable deterioration of performance, occurred for cw powers of two watts, and for pulse energies of 170 ergs. These results show that tunnel diodes can handle approximately one order of magnitude more cw power and pulse energy than conventional point-contact mixer diodes.

Table 4 lists the lowest system noise figures measured to date. For this test, a 30-megacycle amplifier having a 1.7-db noise figure was used. (The quoted single-sideband noise figures include the losses of the image-rejection filters.)

References

34. C. A. Burrus, "Millimeter Wave Esaki Diode Oscillator", *Proc. IRE,* Vol. 48, p. 2024, December, 1960.
35. E. W. Herold, R. R. Bush and W. R. Ferris, "Conversion Loss of Diode Mixers Having Image Frequency Impedance", *Proc. IRE,* Vol. 33, p. 603, September, 1945.
36. H. C. Torrey and C. A. Whitmer, *Crystal Rectifiers,* McGraw-Hill Book Company, Inc., New York, 1948.
37. L. I. Smilen and D. C. Youla, "Stability Criteria for Tunnel Diodes", *Proc. IRE,* Vol. 49, pp. 1206-1207, July, 1961.
38. IRE Standard on Electron Tubes: Definition of Terms, 1957, *Proc. IRE,* Vol. 45, p. 1000, July, 1957.

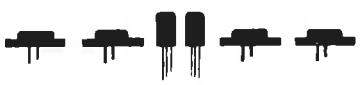

VALVE REPLACEMENT IN SERIES-STRING RECEIVERS

by A. Wardale

AWV Application Laboratory

With the large flow of migrants and visitors into Australia, an appreciable number of imported radio and television receivers have appeared here. Many of these receivers are of the series-string type, that is, the heaters of the valves are connected in series, or sometimes in a series-parallel arrangement, and then fed from a high-voltage source, which is frequently the mains input to the receiver. Ballast resistors may be used to take up the excess voltage.

In some cases, the valves used in such an arrangement are not all rated for the same heater current. One then finds that both series and parallel connections are used, or that some of the heaters that have a lower rated current are shunted with a resistor to carry some of the total current through the system.

As most readers will be aware, this type of arrangement has never been popular in Australia, partly for safety reasons, and there may therefore be many servicemen and technicians who would find such an arrangement puzzling, particularly in the absence of a circuit diagram. Further the increased number of such units now in use here makes the problem of valve replacement increasingly difficult.

It will be appreciated that in a system such as that described, it is not so much a matter of finding a valve with the right heater voltage to act as a replacement, as finding a valve with the right heater current. Further, such sets generally use valves which have been specifically developed for the series-string type of circuit; this often means that replacement of a defective valve, on the face of it, can only be effected with imported types, as the series-string types are not normally made in Australia.

There is one favourable point about all this, and that is the fact that many of the series-string heater type valves are modifications of the more-familiar 6.3-volt and 12.6-volt valves with which we are used to dealing. It may not be generally known that many of the series-string type valves can be easily replaced by their parallel-heater equivalents, by installing a shunt resistor across the heater of the replacement valve, so that the current passed through the replacement heater, plus the current in the shunt resistor, equals the current through the series string.

This can only be done where an equivalent is available having a higher heater voltage and hence a lower heater current. An example is type 12AX4GT, which can be replaced by a 17AX4GT, and either of these two types can be replaced by a 25AX4GT.

The accompanying table shows a list of types that can be replaced in this manner, with the replacement type given and also the value and rating of the resistor required. This listing has been restricted to replacement types which are normally available in Australia.

Where it is desired to make a replacement with a type not listed here, the value of the resistor required can be calculated by dividing the heater voltage of the replacement type by the difference between the heater currents of the original and the replacement type. The wattage rating of the resistor can then be ascertained in the usual E^2/R, E being the heater voltage of the replacement type. In compiling the table, resistors in the 5% preferred range have been chosen, and a similar method could be adopted in selecting other calculated values.

It will be obvious that replacemnt in this way will slightly reduce the current in the string, due to the increased voltage drop across the replacement valve. This will not be serious unless a number of valves is replaced in the same set. If in doubt, the current should be checked, and readjusted to the correct value by adjustment of the series ballast resistor(s).

By way of example, let us assume that a type 5CZ5 has failed, and replacement with a type 6CZ5 is considered. The heater voltage of the 6CZ5 is 6.3; the difference in the heater currents is 0.15 amperes. Then 6.3/0.15 gives us 42 ohms; 43 ohms is the nearest standard 5% value. E^2/R equals 6.3/42, giving the dissipation in the shunt resistor slightly less than 1 watt. The wattage rating given here, and those shown in the table, represent actual dissipation, and the resistor chosen should be derated according to circumstances. Extra care should be used when replacing valves with controlled heater warm-up characteristics.

When servicing ac/dc radio receivers of the older types, it is often difficult to obtain replacement rectifiers. These can be replaced by an AWV silicon diode connected between the plate and cathode pins of the socket with a resistance equal to the original valve heater resistance (hot) connected across the heater pins of the socket. Due to the increased efficiency of silicon diodes, compared with the thermionic valves, it is advisable to connect a 100-ohm resistor in series with the diode. The wattage rating of this resistor should be $500I^2$, where I is the dc current drain of the set in amperes. The diode should be an AWV type 1N1763 for a 110-volt set, and an AWV type AS3 for a 240-volt set.

One final word; it goes without saying that any serviceman who carries out a modification of this kind on a receiver should leave details of the modifications on a tag tied to the chassis, for the assistance of the next man who meets with the set. A few moments spent in this way may save a great deal of time and trouble at a later date, and is the sort of thing that any conscientious man would want to do.

ORIGINAL TYPE	REPLACEMENT TYPE	SHUNT RESISTOR (OHMS)	RESISTOR RATING (WATTS)
2AF4A	6AF4A	16	3
2BN4A	6BN4A	16	3
2CW4	6CW4	20	2
2CY5	6CY5	16	3
2DS4	6DS4	20	2
2EN5*	6AL5	43	1
2FH5	6FH5	16	3
2GK5	6GK5	15	3
3AF4A	6AF4A	27	2
3AL5	6AL5	22	2
3AU6	6AU6	22	2
3AV6	6AV6	22	2
3BA6	6BA6	22	2
3BC5	6BC5	22	2
3BE6	6BE6	22	2
3BN4A	6BN4A	24	2
3BN6	6BN6	22	2
3BU8	6BU8	22	2
3BY6	6BY6	22	2
3BZ6	6BZ6	22	2
3CB6	6CB6	22	2
3CE5	6CE5	22	2
3CF6	6CF6	22	2
3CY5	6CY5	24	2
3DK6	6DK6	22	2
3DT6	6DT6	22	2
3FH5	6FH5	24	2
3GK5	6GK5	24	2
3GS8	6BU8	22	2
4AU6	6AU6	43	1

* Connect pins 1 and 5 together at the socket.

ORIGINAL TYPE	REPLACEMENT TYPE	SHUNT RESISTOR (OHMS)	RESISTOR RATING (WATTS)
4AV6	6AV6	43	1
4BC5	6BC5	43	1
4BC8	6BC8	30	2
4BL8	6BL8	43	1
4BN6	6BN6	43	1
4BQ7A	6BQ7A	30	2
4BS8	6BS8	30	2
4BU8	6BU8	43	1
4BZ6	6BZ6	43	1
4BZ7	6BZ7	30	2
4CB6	6CB6	43	1
4CS6	6CS6	43	1
4CY5	6CY5	62	1
4DE6	6DE6	43	1
4DT6	6DT6	43	1
4EH7	6EH7	43	1
4EJ7	6EJ7	43	1
4ES8	6ES8	27	2
4EW6	6EW6	30	2
4GS8	6BU8	43	1
5AM8	6AM8	43	1
5AN8	6AN8	43	1
5AQ5	6AQ5	43	1
5AS8	6AS8	43	1
5AT8	6AT8	43	1
5BK7A	6BK7A	43	1
5BQ7A	6BQ7A	130	0.5
5BR8	6BR8	43	1
5BW8	6BW8	43	1
5CG8	6CG8A	43	1
5CL8A	6CL8A	43	1
5CM8	6CM8	43	1
5CQ8	6CQ8	43	1
5CZ5	6CZ5	43	1
5EA8	6EA8	43	1
5EU8	6EU8	43	1
5EW6	6EW6	130	0.5
5GH8	6GH8	43	1
5GM6	6GM6	130	0.5
5J6	6J6	43	1
5T8	6T8	43	1
5U8	6U8	43	1
7AU7†	12AU7A†	22	2
9AU7†	12AU7A†	43	1
12AX4GT	17AX4GT	110	3
	25AX4GT	82	10
12BQ6GT	17BQ6GT	110	3
	25BQ6GT	82	10
12DQ6	17DQ6 / 17GW6	110	3
12GW6	17GW6 / 17DQ6B	110	3
17AX4GT	25AX4GT	160	4
17BQ6GT	25BQ6GT	160	4

† Heaters of both sections in parallel.

ANNUAL INDEX, 1963

Editor ..... **Bernard J. Simpson**

Radiotronics is published twelve times a year by the Wireless Press for Amalgamated Wireless Valve Co. Pty. Ltd. The annual subscription rate in Australasia is £1, in the U.S.A. and other dollar countries $3.00, and in all other countries 25/-.

Subscribers should promptly notify Radiotronics, P.O. Box 63, Rydalmere, N.S.W., and also the local Post Office of any change of address, allowing one month for the change to become effective.